International Conference
ENGINEERING MECHANICS 2010
Svratka, Czech Republic, May 10 – 13, 2010

ASSESSMENT OF AILERON TAB INSTALLATION INFLUENCE TO ULTRA-LIGHT AIRCRAFT FLUTTER CHARACTERISTICS

J. Čečrdle*

Summary: *Submitted paper deals with the aileron flutter of the ultra-light aircraft. It gives an assessment of influence of the additional installation of the tab regarding the aircraft aileron flutter characteristics. The necessary actuation system stiffness and the aileron flapping frequency to ensure the stability at the aircraft maximal speed are evaluated. The work was motivated by the M-7 ultra-light aircraft accident in the western Bohemia in 2006. The FE model was prepared by the optimization approach. The design variables were mass and stiffness characteristics, design responses (constrains and objective functions) were given from the ground vibration tests data.*

1. Introduction

In the Czech Republic, there was a considerable growth in development and production of the ultra-light aircraft recently. Nowadays, the modern composite materials and advanced technologies are applied. New generation ultra-light aircraft are lighter, aerodynamically refined and equipped by more powerful engines. It allows installation of advanced equipment (retracting landing gear, navigation devices, towrope etc.). Also flight performances are increasing (maximal speed, rate of climb etc.). In many aspects, ultra-light aircraft expand to the very-light aircraft category. However, the ultra-light aircraft are not certified under the state certification authority in the Czech Republic. Except the formal flight flutter test, there are no aeroelastic or modal analyses or experiments required for the ultra-light aircraft certification. Also a home-made alteration of the structure is a typical practice. In the last time, there came up

Figure 1 M-7 "Ornis" aircraft

* Ing. Jiří Čečrdle, Ph.D.: Výzkumný a zkušební letecký ústav a.s., Beranových 130; 199 05 Praha - Letňany; tel.: +420.225 115 123, fax: +420.283 920 018; e-mail: cecrdle@vzlu.cz

several ultra-light aircraft accidents with the probable cause specified as the dynamic instability (flutter). Thus, some kind of simplified aeroelastic certification requirement for the ultra-light aircraft can be expected in the future.

2. Motivation

In the May 2006, the M-7 "Ornis" ultra-light aircraft accident occurred in the western Bohemia. M-7 "Ornis" (fig.1) is a two-seat single-engine strut high-wing aircraft with the wingspan of 10.42 m; length of 6.16 m and maximal take-off weight of 450 kg.

During the flight, both ailerons and outer part of one half-wing had broken away. Then the aircraft crashed down and flamed up. Both two people on board have been killed. During the investigation of the accident, the examination of the aircraft wreckage, hearing of involved people, simplified modal test and flutter calculations have been performed. As the probable cause, the aileron flutter instability was assessed (AAII (2006)).

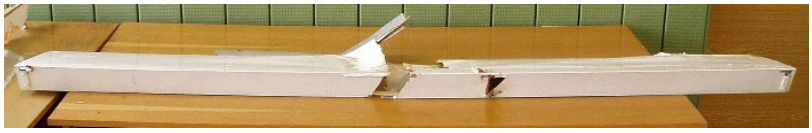

Figure 2 Right aileron overall view

Figure 3 Trim tab – bottom view

Figure 4 Trim tab – top view

Let us pay focus to the following matter of facts. Closely before the accident, the original engine was replaced by the other, more powerful one (Rotax 912S) with the longer-diameter wooden propeller (SR 30S), so that the aircraft could be able to draw along gliders. Before the accident, the aircraft covered only 13.5 flight hours with the new engine system. On the starboard aileron (fig.2), there was found the fixed trim tab (fig.3 and 4) made of a duralumin plate screwed to the bottom part of the aileron trailing edge. There were bolts with different bolt-heads and lengths used. Also there was a visible boundary trace of the epoxide-like matter on the top side (fig.5). The tab installation looks like the home-made amateurish replacement of the former one (see Růžek and Běhal (2006)).

Figure 5 Epoxide-like boundary

Due to these facts, it may enter to one's head the hypothesis that the tab was installed after the engine change, e.g. to eliminate the higher gyroscopic moments of the propulsion system, despite that the aircraft owner did not confirm this.

The ailerons have no balancing mass. The aileron centre of gravity was behind the hinge axis, it means that the ailerons were statically under-balanced. With respect to the aileron mean geometry chord, the level of under-balancing was 35.9%. Added mass of the tab increased the under-balancing level by 3.7%. Moreover, considering the aileron actuation system stiffness retained, it caused a decreasing of the aileron flapping frequency. Regarding the aeroelastic stability, the both mentioned facts are considered as destabilizing. To analyze the level of the mentioned effect is the subject of the presented work.

3. Analytical Model Preparation

In the aeroelastic analysis, there are two main analytical approaches. The first one is the direct usage of the ground vibration tests results as an input data to the flutter calculations. The advantage of this approach is that the input data has direct relation to the reality and there is no demand of the structural data. This fact is very useful for the ultra-light aircraft, since there are usually poor or even no structural data available. Such approach is usually used for the aeroelastic check analyses. On the other side, the analyses are limited by the configurations, which were analyzed by the tests.

Provided there are parametric studies and evaluation of the specific parameter influence required, it is necessary to apply the second approach, which is based on the finite element (FE) analysis. It allows changing of any structural parameter; however the structural (mass, stiffness) data to prepare the model are required. In case, there are no data available, it is possible to utilize the results of the tests (static tests, ground vibration tests). Structural parameters are then tuned to these results by means of the optimization based method.

The following text describes the methodology how to build a model of a trapezoidal shaped wing.

Aerodynamic model for simulation of the non-stationary aerodynamic forces consists of the flat panels. Geometry to build such model is mostly at disposal; otherwise it is possible to measure it directly on the aircraft.

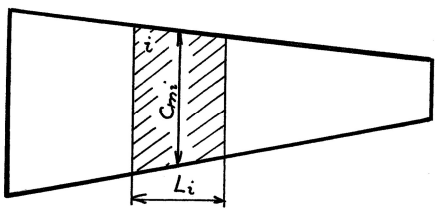

Figure 6 Wing geometry explanation

Inertia model is represented by lumped mass elements. The total mass is expected to be known, otherwise can be measured. The position of the centre of gravity axis, unless is known as well, can be estimated at the 40% of the wing chord. According to Smrček (1961) and Maleček (1964), considering the geometry, the initial mass distribution can be estimated as:

$$m_i = m' \; c_{mi}^2 \; L_i \tag{1}$$

Where m_i is mass of the i-th wing segment, other geometry is obvious from fig.6. The wing relative mass is given by:

$$m' = \frac{3}{4} \; \frac{M\left(1 + 2\,\lambda + \lambda^2\right)}{S\,c_m\left(1 + \lambda + \lambda^2\right)} \tag{2}$$

where M is the wing total mass, S is the wing area and c_m is the wing middle chord and finally, λ is the wing taper ratio.

Considering one-spar wing the initial mass moment of inertia will be given by:

$$J_{mi} = \left(\sigma_i^2 + (0{,}28\, c_{mi})^2\right) m_i \tag{3}$$

where σ is the distance of the elastic and centre of gravity axes.

Stiffness model is represented by the mass-less beam placed at the elastic axis. The position of the elastic axis, unless is known as well, can be placed to the position of the main spar. Considering the geometry, the initial area inertias distribution for the both bending and torsion are proportional to the:

$$(I_{xi}, I_{ki}) \approx c_{mi}^4 \tag{4}$$

The value of the stiffness is then realized by means of the modulus E and G respectively.

The initial model is then optimized in order to match the available experimental results. Design variables are represented either by the stiffness or mass parameters. Stiffness parameters on the global level, it means that the same changes for whole wing (scale factor) are represented by values of E and G modulus respectively. Stiffness parameters on the local level are represented by values of area inertias. Also specification of other stiffness parameters modeled by spring elements (spring stiffness factor) are possible to be specified (e.g. wing strut stiffness). Mass design variables are represented by values of mass and mass moments of inertia. Obviously, the lower and upper bounds of design variables can be set. Also, the linking among the design variables which makes the change of dependent design variable as a linear combination of specified independent design variables is possible:

$$x_d = C_0 + C_{MULT} \sum_i C_i\, x_i \tag{5}$$

It is clear, that the parameters which are known (e.g. control surface mass) must not be selected as design variables.

Design responses may become either design constrains or an objective function. It may become either linear or nonlinear function of other design responses, design variables, properties, constants, discrete values etc.

Design constraints define the limitations of the optimization in the design space. Generally, the stricter constraints lead to worse result in terms of the objective function value, but the physical interpretation of the final design variables is better, and vice versa. For example, constraints can limit the stiffness or mass descent from the root to the tip, root and tip stiffness ratio, to keep the known total mass etc. Also, during the optimization, it is worth to constrain the value of parameters included in the objective function so as not to get worse during the next phase of the optimization process.

Objective function is a scalar value, which is minimized. It incorporates the target values (experimental results) to be matched.

Firstly, it may consider the relative error in the natural frequency as:

$$\left\{\varepsilon_f\right\} = \left\{\frac{f_{FEA} - f_{GVT}}{f_{GVT}}\right\} \tag{6}$$

Where the subscripts FEA and GVT represent the FEM model and ground vibration test data respectively. The objective function is then expressed as weighted squared minimization as:

$$min\left(\left\{\varepsilon_f\right\}^T\left[W_f\right]\left\{\varepsilon_f\right\}\right) \tag{7}$$

The weighting factor is represented by matrix $[W_f]$ reflecting the confidence in the test data. In a similar way, the relative error in modal displacements can be considered as well, e.g. the weighted squared minimization of relative error in the bending modes node point position in the spanwise direction etc.

Other way, how to express the error in the mode shapes is the usage of correlation criteria e.g. Modal Assurance Criterion (MAC), which is defined as:

$$MAC\left(\Psi_a,\Psi_e\right)=\frac{\left|\left(\left\{\Psi_a\right\}^t\left\{\Psi_e\right\}\right)\right|^2}{\left(\left\{\Psi_a\right\}^t\left\{\Psi_a\right\}\right)\left(\left\{\Psi_e\right\}^t\left\{\Psi_e\right\}\right)} \tag{8}$$

The MAC values can be included by the weighted MAC function as:

$$min\left(\left[W_{MAC}\right]\left\{1-\left[MAC\right]\right\}\right) \tag{9}$$

The weighting is represented by matrix $[W_{\mathrm{MAC}}]$, the MAC values for optimization are computed only from the limited set of "key" nodes of the FE model.

The optimization process of the mentioned objective function make the parameters changes with no matter regarding the magnitude or sign. It may lead to the model which may not be representative to the physics of the aircraft. Thus, the minimization process should include also the demand to minimize the changes of design variables, especially those ones, which are considered as reliable. The changes of parameters are defined as:

$$\left\{\Delta p\right\}=\left\{\frac{p-p_0}{p_0}\right\} \tag{10}$$

where p is the final parameter value and p_0 the initial one. Final objective function including the mentioned sections may become:

$$min\left(\left\{\varepsilon_f\right\}^T\left[W_f\right]\left\{\varepsilon_f\right\}+\left\{W_{MAC}\right\}^T\left\{1-\left[MAC\right]\right\}+\left\{\Delta p\right\}^T\left[W_p\right]\left\{\Delta p\right\}\right) \tag{11}$$

The weighting factor for parameters is represented by matrix $[W_{\mathrm{p}}]$. Obviously the objective function may include also the static test results, e.g. relative errors of static displacements. The optimization may include multiple solutions (static, normal modes, flutter etc.).

Optimization is usually performed in several steps. During each step, we use specific type of design variables with appropriate constraints and objective functions. Possible approach is for example:

First of all to make the

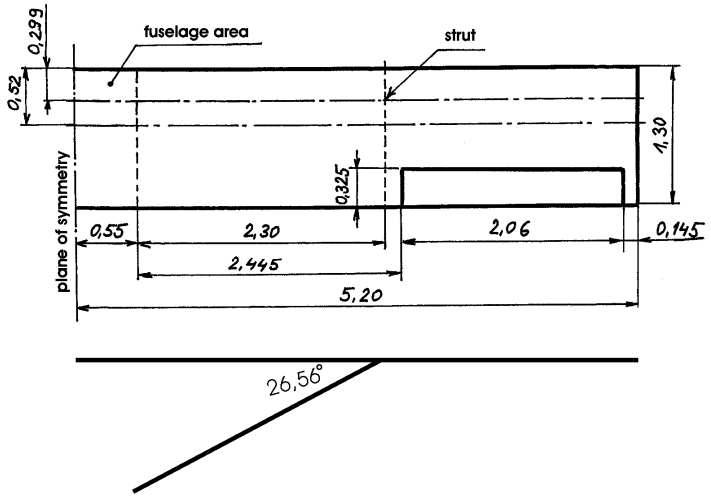

Figure 7 M-7 aircraft wing geometry

rough tuning of the stiffness parameters by means global beam stiffness and spring constants to natural frequencies, secondly to perform the beam local stiffness tuning to the static displacements, then the mass parameters tuning to the natural frequencies and finally local stiffness tuning to the mode shapes.

Table 1 GVT results summary (Weigel (2009))

title	abbr.	natural frequency	damping ratio	node at % of half-span
		f_0 [Hz]	α [%]	
1st symmetric bending	1.SWB	11.7	1.70	48
1st antisymmetric bending	1.AWB	16.3	3.53	77
2nd symmetric bending	2.SWB	21.1	1.97	59
1st symmetric torsion	1.SWT	26.6	4.48	
2nd antisymmetric bending	2.AWB	40.7	2.57	80
2nd symmetric torsion	2.SWT	41.8	2.32	
2nd antisymmetric torsion	2.AWT	56.1	1.75	

For the preparation of the M-7 aircraft wing FE model, the following input data were available:

Wing geometry – see fig.7; from Pechanec (1996) were obtained the elastic axis position at 23% of chord; center of gravity axis position at 40% of chord; wing total (full-span) weight of 50 kg; aircraft total weight (selected configuration - including fuel and a pilot) of 365.3 kg. Aircraft center of gravity at 23.53% of wing chord and 0.357 m below the wing.

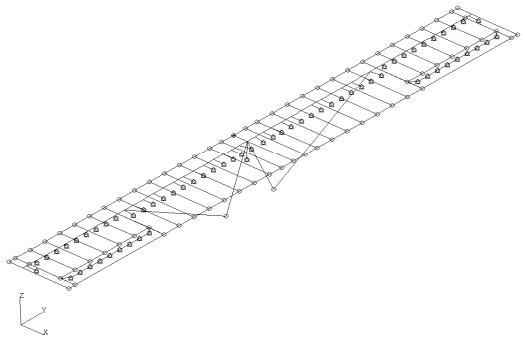

Figure 8 M-7 aircraft wing FE model

From the static test, there were a data regarding loads and corresponding wing tip displacements. Nevertheless, considering the unreliably described work points of the load components, these data did not be utilized. After the accident, there were performed the mass measurements of the aileron as described in Maleček and Hlavatý (2006). From these measurements the aileron inertia parameters were gained (total mass of 1.97 kg; mass moment of inertia with respect to aileron pivot axis of 0.055845 kg.m^2; center of gravity position 0.117 m behind the pivot axis and 1.035 m from the aileron root rib). From the other same type aircraft ground vibration test, the natural frequencies and positions of node points summarized in the tab.1 were gained.

FE model was built as a full-span respecting the known input data and the rules for initial stiffness and mass parameters. The aileron inertia characteristics were incorporated in order to keep the initial inertia parameters of the entire wing structure. The FE model is demonstrated in the fig.8. Aerodynamic model for Doublet - Lattice Theory was prepared respecting the outline of the wing, aileron, hinge etc. The aerodynamic mesh was refined around leading or trailing edges as well as in the aileron area.

Updating of the FE model was performed in several phases. The aileron actuation was blocked during the optimization. It corresponds to the state of the GVT. The initial values of the E and G modulus, and also the strut stiffness were set guessingly. During the optimization,

Table 2 Final model frequencies and comparison with the GVT

title	abbr.	GVT	FE model – final		
		f_{0GVT} [Hz]	#	f_{0FEA} [Hz]	$\|(\Delta f_0/f_{0GVT})\|$ [%]
1st symmetric bending	1.SWB	11.7	1	11.794	0.8
1st antisymmetric bending	1.AWB	16.3	2	16.193	0.6
1st antisymmetric torsion	1.AWT	---	3	17.079	---
2nd symmetric bending	2.SWB	21.1	4	22.702	7.6
1st symmetric torsion	1.SWT	26.6	5	26.471	0.5
2nd antisymmetric bending	2.AWB	40.7	6	41.063	0.9
3rd symmetric bending	3.SWB	---	7	44.735	---
2nd symmetric torsion	2.AWT	56.1	8	57.192	1.9
2nd antisymmetric torsion	2.SWT	41.8	9	59.063	41.3

the design variables, design constrains and the objective functions were adjusted in order to keep the previously reached congruence of frequencies. The level of model improvement was measured by the relative change in the objective function:

$$\Delta OBJ = \frac{OBJ_{INIT} - OBJ_{FINAL}}{OBJ_{INIT}} . 100 \ [\%] \tag{12}$$

For the design variables, there were used global stiffness parameters, strut stiffness, local stiffness parameters, mass and moments of inertia. Design constraints defined the condition to keep the total mass, descent character of the stiffness distribution and also the stiffness difference among the elements. The objective functions included the relative differences in the natural frequencies, positions of the node points and changes of the parameters.

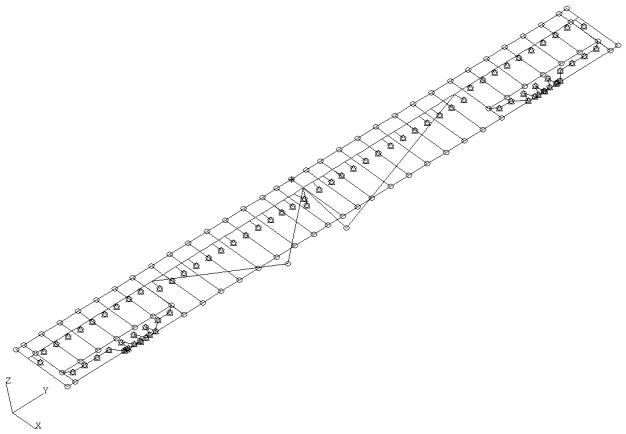

Figure 9 M-7 aircraft wing FE model including the tab

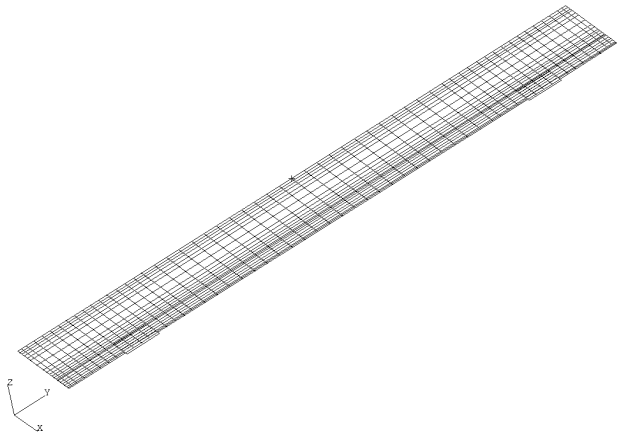

Figure 10 Aerodynamic model including the tab

The final model frequencies are listed in tab.2. The agreement to the GVT is indeed satisfactory. The high difference of the mode 2.SWT is not critical, since this mode is not expected to make a decisive influence to the flutter stability. The described model was used as a reference model ("no tab" configuration).

Afterwards, the tab inertia characteristics were included to the mentioned reference model. Each component of the tab (tab plate, cover plates, screws with nuts) was modeled by separate mass elements. Mass values were given from the weighing of the components, mass moments of inertia and elements positions were given from the geometry. The structural model including the tab is presented in fig.9. Regarding the aerodynamic model, the two option models were prepared, the first one with the same aerodynamic model as the reference model (neglecting the aerodynamic effect of the tab), the second one including the aerodynamic effect of the tab (increasing of the wing area). The latter model is presented in fig.10.

4. Analyses Description and Results

Flutter analyses were performed using mentioned three variants of the model:

1) no tab configuration (reference model)
2) tab configuration, tab aerodynamic effect neglected
3) tab configuration, tab aerodynamic effect included

Flutter calculations were performed by the PK method:

$$\left[M_{hh} p^2 + \left(B_{hh} - \frac{1}{4} \frac{\rho c V Q_{hh}^{\mathrm{Im}}}{k} \right) p + \left(K_{hh} - \frac{1}{2} \rho V^2 Q_{hh}^{\mathrm{Re}} \right) \right] \{u_h\} = 0 \tag{13}$$

$$p = \omega(\gamma \pm j) = p^{\mathrm{Re}} + j p^{\mathrm{Im}} \tag{14}$$

There were following analysis parameters considered: Mach number $M = 0$ (no correction to compressibility), air density ρ = 1.225 kg.m^{-3} (flight altitude $H = 0$); velocity range from 10 m.s^{-1} to 150 m.s^{-1}. Analyses included 11 mode shapes (tab.2 modes and both symmetric and antisymmetric aileron flapping modes). The common value of the structural damping ($\alpha = 0.01$) was used. The aileron drive stiffness varied from 5.0 Nm.rad^{-1} to 2700 Nm.rad^{-1}. There is demonstrated influence of the tab additional mass in fig.11 (example for the antisymmetric aileron flapping). There is noticeable the decreasing of the flapping frequency due to additional tab mass. This effect may be quite significant, up to almost 30%.

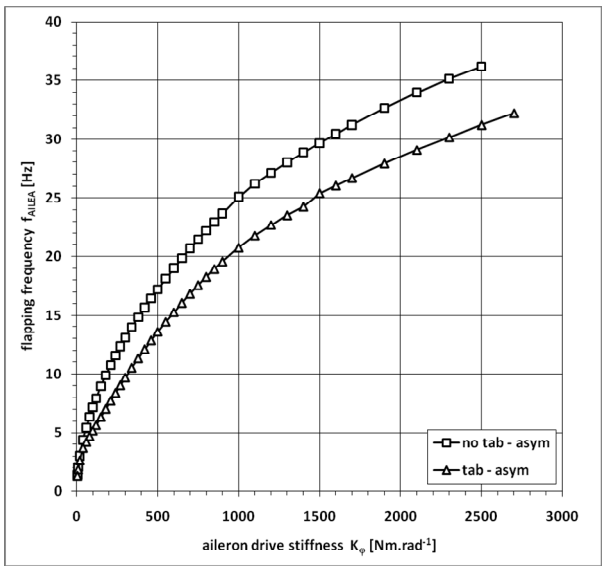

Figure 11 Aileron drive stiffness vs. antisymmetric flapping frequency

There were the following types of the flutter instability found; all of these instabilities have the critical combination of two modes:

Symmetric bending aileron flutter (critical combination of 1st symmetric bending and aileron flapping) with the critical flutter frequency of

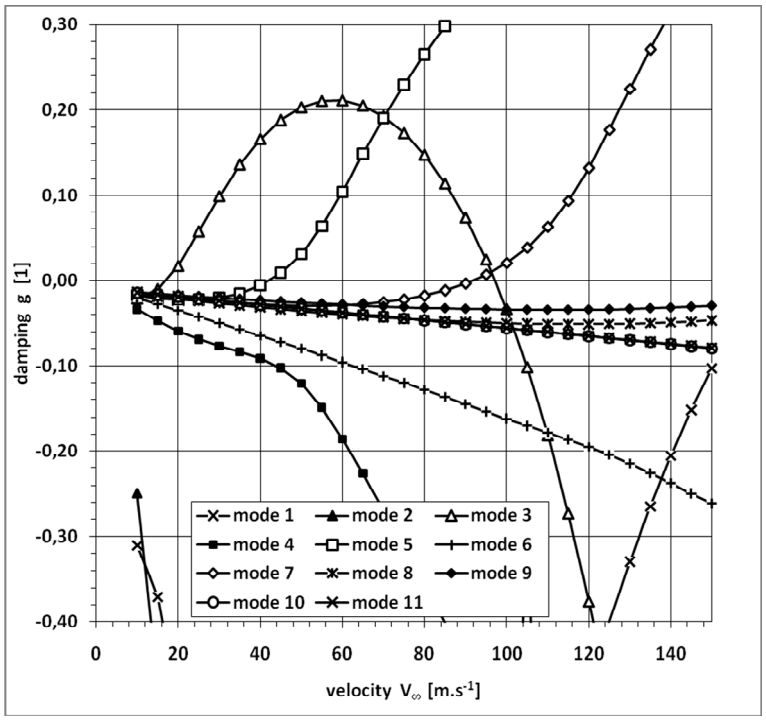

Figure 12a V – g diagram – example ($K\varphi$=150 Nm.rad^{-1}, no tab)

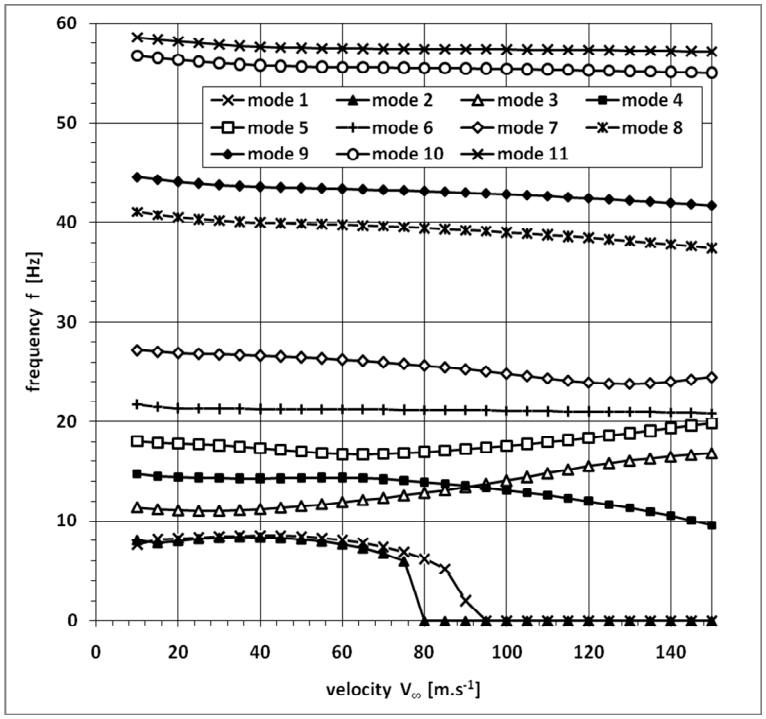

Figure 12b V – f diagram – example ($K\varphi$=150 Nm.rad^{-1}, no tab)

(10.0 - 12.0) Hz. The minimal values of the critical flutter speed are reaching the velocity of 15 m.s^{-1}.

Antisymmetric torsional aileron flutter (critical combination of 1st antisymmetric torsion and aileron flapping) with the critical flutter frequency of (16.0 - 22.0) Hz. The minimal values of the critical flutter speed are reaching the velocity of 40 m.s^{-1}.

Symmetric torsional aileron flutter (critical combination of 1st symmetric torsion and aileron flapping) with the critical flutter frequency of (25.0 - 28.0) Hz. The minimal values of the critical flutter speed are reaching the velocity of 85 m.s^{-1}.

The example of the V-g-f diagram is in fig.12. It represents the calculation for "no tab" configuration and the aileron actuation stiffness of K_φ=150 Nm.rad^{-1}. There appeared all mentioned types of instability. Summary of the flutter speed for all three models as a function of the aileron flapping frequency and aileron drive stiffness is presented in fig.13 and fig.14 respectively.

5. Assessment of Results

Installation of the tab resulted into the following consequences:

1) Decreasing of the aileron flapping frequency

Considering no change in the aileron actuation system stiffness, the additional mass caused decreasing of the aileron flapping frequency. In general, in terms of the flutter behavior, such change has negative influence. Control surfaces flapping mode frequency is ordinarily increasing with the flow velocity (aerodynamic stiffness). Provided the initial frequency for zero airflow velocity became lower, the flapping mode frequency may couple and cause instability with additional wing modes crossing their frequencies increasing the airflow velocity.

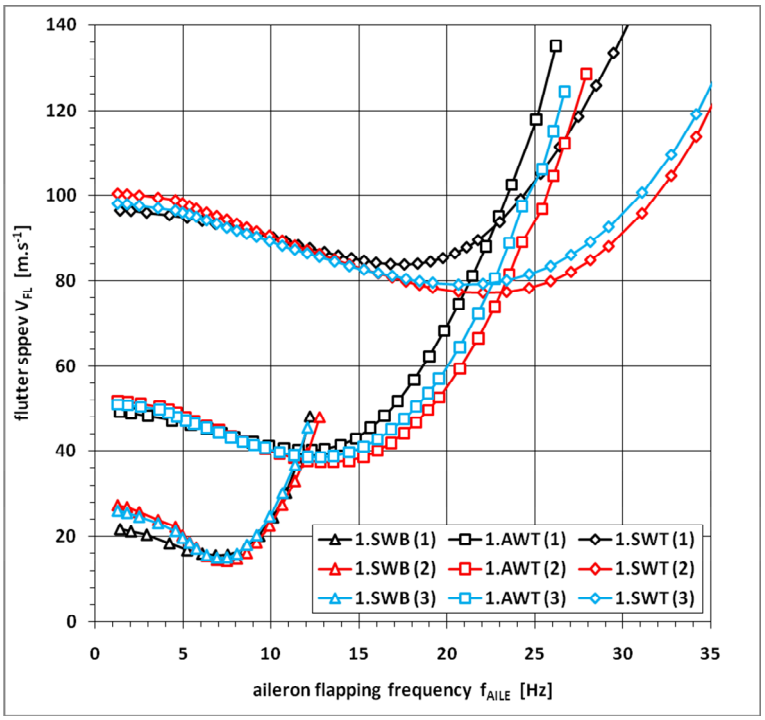

Figure 13 Critical flutter speed vs. aileron flapping frequency: (1) – no tab; (2) – tab; (3) – tab (aerodynamic included)

2) Increasing of aileron under-balancing

Additional mass moves the aileron center of gravity backwards; it means the static under-balancing is increasing. In general, in terms of the flutter behavior, such change has destabilizing effect as well. Considering the bending – torsion aileron flutter, the additional mass on the trailing edge makes in most cases increase of the cross inertia with respect to the wing mode node line and the pivot axis. Provided the flapping frequency is lower than the coupled wing

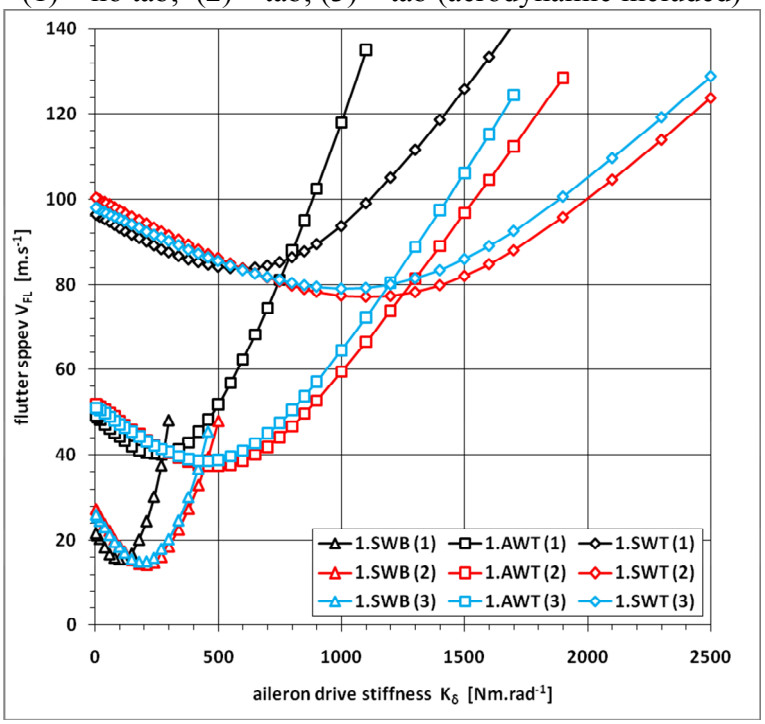

Figure 14 Critical flutter speed vs. aileron actuation stiffness: (1) – no tab; (2) – tab; (3) – tab (aerodynamic included)

mode, it makes increase of the dynamic under-balancing with negative consequence to the flutter stability.

3) Additional aerodynamic surface

Increase of the aileron surface due to the tab over the aileron outline causes increasing of the aileron aerodynamic force. Provided the aileron flapping frequency is lower than the coupled wing mode frequency, the effect is destabilizing and vice versa.

Following the given description, the probable influence of the tab installation to the flutter stability can be estimated as destabilizing (see also Tempelton (1954)). According the aircraft documentation, the maximal flight speed with the new engine and propeller was $V_{NE} = 170$ km.h^{-1} (47.2 m.s^{-1}). Let us consider this velocity as a reference for assessment. The aileron flapping frequency calculated from the control system stiffness test performed in 1994 and the aileron mass measurements is $f_{AILE} = 16.6$ Hz. From the given documentation, it cannot be decided, whether this value represents the symmetric or antisymmetric rotation. As a clue we used the GVT results of the other type of the ultra-light aircraft (ŠK-1 "Trempík") performed at the VZLU in 1980 (see Černý (1980)). ŠK-1 is the similar aircraft structure (high-wing strut) with comparable dimensions, materials and weights. There were measured the symmetric aileron flapping frequency of 33.67 Hz and antisymmetric one of 14.68 Hz. Considering this, we can estimate the M-7 aircraft flapping frequency of 16.6 Hz as the antisymmetric one. Regarding these facts, we can formulate the following statements:

We consider the aileron drive system with no failure or extreme backlash. Thus 1.SWB instability is not presumable considering the high value of the symmetric flapping frequency. Furthermore, for the 1.AWB instability, we can assume the $f_{AILEA} < 4.8$ Hz as not presumable as well. Finally, the flutter speed of the 1.SWT instability does not reach the reference velocity (47.2 m.s^{-1}).

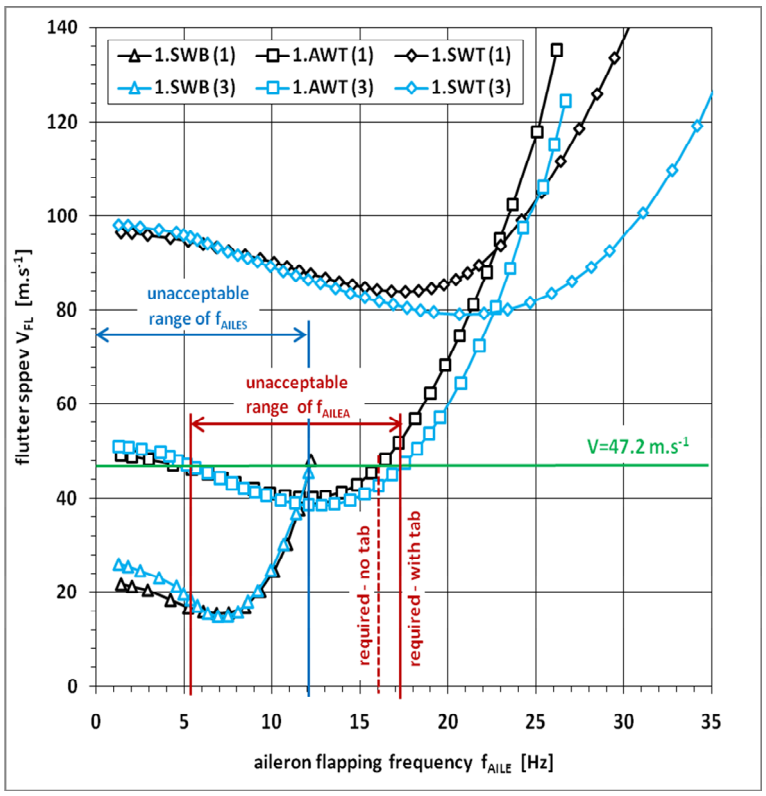

Figure 15 Required aileron flapping frequencies
(1) – no tab; (3) – tab (aerodynamic included)

For the configuration with no tab, the requirement of stability in terms of the minimal aileron antisymmetric flapping frequency is $f_{AILEA} > 16.0$ Hz, the corresponding minimal aileron actuation system stiffness condition is $K_\delta > 440$ Nm.rad^{-1}.

For the configuration with tab (considering the influence of aerodynamics), the requirement of stability in terms of the aileron antisymmetric flapping frequency is $f_{AILEA} > 17.2$ Hz, the corresponding minimal aileron actuation system

stiffness condition is $K_\delta > 720$ Nm.rad^{-1}. The described statements are illustrated in fig.15 and fig.16.

6. Conclusion

From the described analyses, it is obvious, that the level of reserve in terms of the flutter stability was low, even for configuration with no tab. It evidences, that the flutter stability issues are relevant also for the ultra-light aircraft category, despite that their operational velocities are quite low.

The retrofitting of the aileron tab had destabilizing effect in terms of the flutter. The static under-balancing of the aileron increased by 3.7 %. To ensure the flutter stability at the maximal velocity of $V_{NE} = 47.2$ m.s^{-1}, the minimal aileron antisymmetric flapping frequency requirement increased by 7.5%, the minimal necessary aileron actuation system stiffness increased even by 63.6%. The retrofitting of the aileron tab might significantly influence the stability of the aircraft, despite that the total mass of the tab was only 0.12 kg.

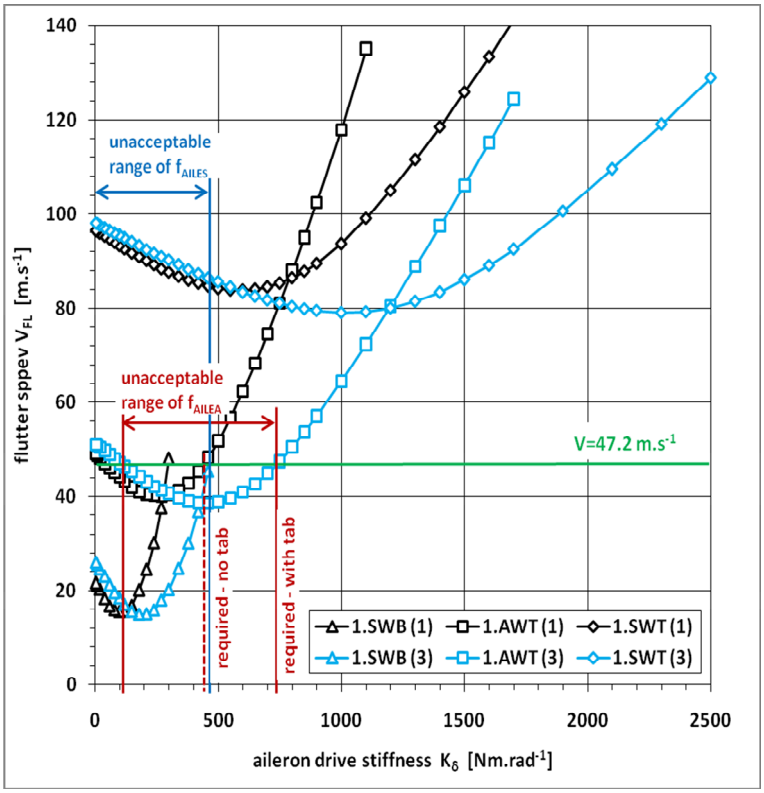

Figure 16 Required aileron actuation stiffness
(1) – no tab; (3) – tab (aerodynamic included)

7. Acknowledgement

The paper was created in the frame of the project MSM 0001066903 “Research on Strength of Low-weight Structures with Special Regard to Airplane Structures” funded from the Ministry of Education, Youth and Sports of the Czech republic.

8. References

Tempelton, H. (1954) *Massbalancing of Aircraft Control Surfaces*, Chapman & Hall Ltd., London

Smrček, M. (1961) *Design of Aeroelastic Models to Compare Flutter Calculation Methods with Experiment (in Czech)*, VZLU a.s. Prague, Report no.V 559/61

Maleček, J. (1964) *Design of 3ST Aeroelastic Model Set (in Czech)*, VZLU a.s. Prague, Report from 2.11.1964

Černý, O. (1980) *Ground Vibration Test of ŠK 1 Aircraft (in Czech)*, VZLU a.s. Prague, Report no. Z-2570/80

Pechanec, V. (1996) *Protocol from Aircraft Weighting, 28.8.1996, aircraft: M-7 no.003 (in Czech)*

Maleček, J. – Hlavatý, V. (2006) *M-7 Ornis Aircraft Aileron Mass Measurement (in Czech)*, VZLU a.s. Prague, Protocol from 3.6.2006

Růžek, R. – Běhal, J. (2006) *Assessment of Destruction Character of M-7 Ornis Aircraft Ailerons and their Suspension*, VZLU a.s. Prague, Report no. R-3903/06

AAII (2006) *Final Report, Investigation into the Incident of Aircraft M 7 ORNIS at Chodovska Hut on 11 May 2006*, Air Accidents Investigation Institute, Czech republic, ref.no.157/06/ZZ

Weigel, K. (2009) *Development of Research Laboratory for Investigation of Light Aircraft Frequency Characteristics with an Emhasis on Aeroelastic Analysis*, Ph.D. Thesis, Czech Technical University, Prague

MSC.Software (2009) *MSC.NASTRAN Documentation Set*